SCIENTIFIC REPORTS

OPEN

SUBJECT AREAS:
ANXIETY
PATHOGENESIS
GENETIC ENGINEERING
METABOLIC DISORDERS

Received
4 April 2013

Accepted
28 May 2013

Published
13 June 2013

Correspondence and requests for materials should be addressed to N.N. (noriyuki@nms.ac.jp)

* These authors contributed equally to this work.

Antioxidant enzyme, 3-mercaptopyruvate sulfurtransferase-knockout mice exhibit increased anxiety-like behaviors: a model for human mercaptolactate-cysteine disulfiduria

Noriyuki Nagahara[1]*, Masatoshi Nagano[2]*, Takaaki Ito[3], Kenji Shimamura[4], Toshio Akimoto[5] & Hidenori Suzuki[2]

[1]Isotope Research Center, Nippon Medical School, 1-1-5 Sendagi, Bunkyo-ku, Tokyo 113-8602, Japan, [2]Department of Pharmacology, Nippon Medical School, 1-1-5 Sendagi, Bunkyo-ku, Tokyo 113-8602, Japan, [3]Department of Pathology and Experimental Medicine, Graduate School of Medical Science, Kumamoto University, 1-1-1 Honjo, Chuo-ku, Kumamoto 860-8556, Japan, [4]Department of Brain Morphogenesis, Division of Organogenesis, Institute of Molecular Embryology and Genetics, Kumamoto University, 2-2-1 Honjo, Chuo-ku, Kumamoto 860-0811, Japan, [5]Division of Laboratory Animal Science, Nippon Medical School, 1-1-5 Sendagi, Bunkyo-ku, Tokyo 113-8602, Japan.

Human mercaptolactate-cysteine disulfiduria (MCDU) was first recognized and reported in 1968. Most cases of MCDU are associated with mental retardation, while the pathogenesis remains unknown. To investigate it, we generated homozygous 3-mercaptopyruvate sulfurtransferase (MST: EC 2.8.1.2) knockout (KO) mice using C57BL/6 embryonic stem cells as an animal model. The MST-KO mice showed significantly increased anxiety-like behaviors with an increase in serotonin level in the prefrontal cortex (PFC), but not with abnormal morphological changes in the brain. MCDU can be caused by loss in the functional diversity of MST; first, MST functions as an antioxidant protein. MST possessing 2 redox-sensing molecular switches maintains cellular redox homeostasis. Second, MST can produce H_2S (or HS^-). Third, MST can also produce SO_x. It is concluded that behavioral abnormality in MST-KO mice is caused by MST function defects such as an antioxidant insufficiency or a new transducer, H_2S (or HS^-) and/or SO_x deficiency.

3-Mercaptopyruvate sulfurtransferase (MST) catalyzes the reaction from mercaptopyruvate ($SHCH_2C(=O)COOH$) to pyruvate ($CH_3C(=O)COOH$) in cysteine catabolism. MST is widely distributed in prokaryotes and eukaryotes[1]. Interestingly, MST is localized in the cytoplasm and mitochondria, but not all cells contain MST[2]. In our studies of the structure–function relationship, we found that a disulfide bond between the dimeric MST, which regulated a monomer (active form)-dimer (inactive form) equilibrium[3,4]. The dimer is formed via an intersubunit disulfide bond by oxidation of exposed cysteine residues on the surface of 2 subunits. This disulfide bond serves as a thioredoxin-specific molecular switch[3,4]. On the other hand, a catalytic-site cysteine is easily oxidized to form a low-redox-potential sulfenate, resulting in loss of activity[4,5]. Then, thioredoxin can uniquely restore the activity[4,5]. Thus, a catalytic site cysteine contributes to redox–dependent regulation of MST activity serving as a redox-sensing molecular switch. These findings suggest that MST serves as an antioxidant protein and partly maintain cellular redox homeostasis. Further, Shibuya et al proposed that MST can produce hydrogen sulfide (H_2S) by using a persulfurated acceptor substrate[6]. As an alternative functional diversity of MST, we recently demonstrated in vitro that MST can produce sulfur oxides (SO_x) in the redox cycle of persulfide ($-S-S^-$) formed at the catalytic-site cysteine of the reaction intermediate[7]. To elucidate these functional diversity of MST in living organism, we tried to generate homogynous (null)

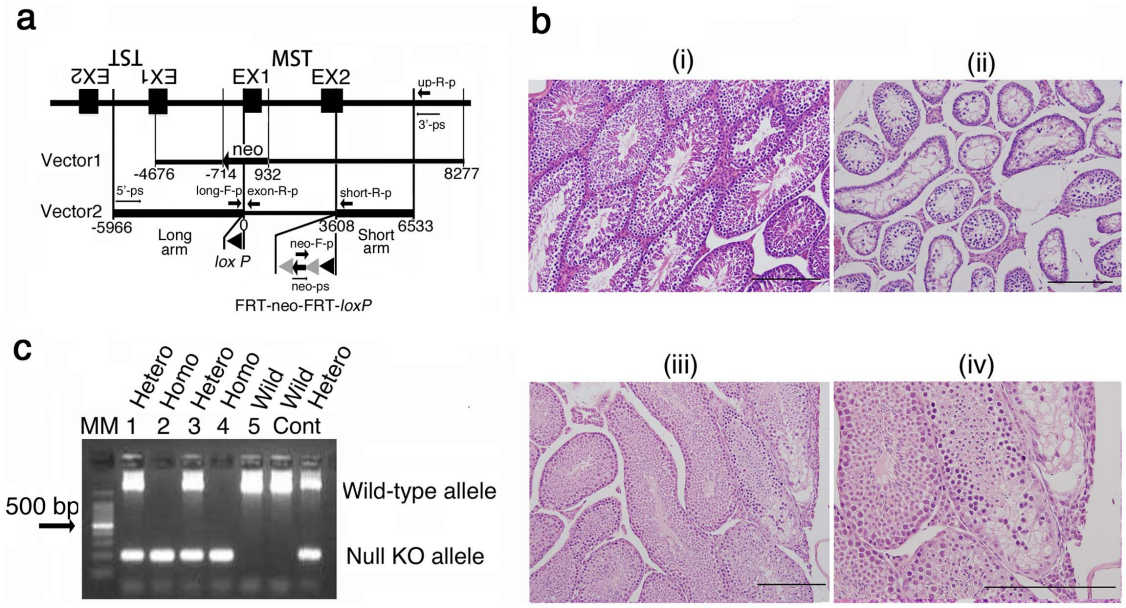

Figure 1 | MST-knockout mice production. (a) The targeting vector, Vector 1 and Vector 2 were designed for generating a conventional and a conditional KO mouse, respectively. A *loxP* sequence and an FRT-neo-FRT-loxP sequence were inserted at the initiation codon, ATG and 3608 bp from the ATG, respectively in EX2. The Cre/*loxP* site-specific recombination system was applied. An ES cell line derived from C57BL/6 mice was used. neo, neomycin resistance gene; exon-R-p, a reverse probe on the EX1 for PCR genotyping; long-F-p, a forward probe on the long arm for PCR genotyping; neo-F-p, a forward probe on the neo for PCR genotyping; Up-R-p, a reverse probe on the upstream of the short arm for PCR genotyping; short-R-p, a reverse probe on the short arm for PCR genotyping; 3′-ps, a forward probe on the long arm for Southern analysis; 5′-ps, a reverse probe on the upstream of the short arm for Southern analysis; neo′-ps, a forward probe on the neo for Southern analysis. (b) Pathologic findings (HE staining) of the testis of a heterozygous KO (Cre+) mouse. (i), normal testis (a wild-type); (ii) and (iii) abnormal testis (mouse ID#44-T-3-2 and #44-3-11-6-T-1, respectively); (iv), a magnified view of (iii). Bars, 200 μm. (c) PCR genotyping of offspring produced from mating between heterozygous KO (Cre−). Genomic DNA was obtained from #44-T-7-3-4-1 (male heterozygous), #44-T-7-3-4-2 (male homozygous), #44-T-7-3-4-3 (female heterozygous), #44-T-7-3-4-4 (female homozygous), and #44-T-7-3-4-5 (female wild-type) (lanes 1 to 5, in the above order). MM, 100-bp DNA ladder molecular marker; Cont, control genome; Hetero, heterozygous KO mouse; Wild, wild-type mouse.

MST-knockout (MST-KO) mouse which was a animal model of mercaptolactate-cysteine disulfiduria (MCDU)[8–16]. MCDU was first recognized and reported in 1968[8] as an inherited metabolic disorder caused by congenital MST insufficiency or deficiency. Most cases were associated with mental retardation[8–13,15], while the pathogenesis remains unknown. In the present study, we revealed by means of comprehensive pathologic, morphologic and functional analyses that MST-KO mice, these mice showed increased anxiety-like behaviors as higher brain dysfunction associated with increase in serotonin level in the brain.

Results

Heterozygous KO mice production. When we previously tried to generate conventional KO mice[17], we did not obtain heterozygous KO mice, probably because gene targeting was extended to the promoter region (−714 bp from the initiation codon ATG) (Fig. 1a). This gene in the germ line may cause an embryonic lethal phenotype, because cytosolic and mitochondrial MST are evolutionarily related to mitochondrial rhodanese[18,19], and these genes lie adjacent to each other on chromosome 15 (NC_000081) and these enzymes act compensatory. In the targeting system, both MST and rhodanese could not be expressed, and therefore, the defect in these 2 family proteins could not be compensated. Thus, the targeting vector had to be improved (Fig. 1a).

To generate conditional and/or null KO mice, the Cre/*loxP* site-specific recombination system was applied for gene targeting in C57BL/6 embryonic stem (ES) cells[17,20,21]. Heterozygous *loxP* site knock-in mice with or without a neomycin resistance gene (*neo*) showed apparently normal development and no abnormalities in morphology. After *in vivo* Cre recombinase treatment of flox mice (by mating with whole tissue expression transgenic mice), the resultant heterozygous (null) KO mice carrying the Cre cassette showed apparently normal development. However, macroscopic and microscopic analysis revealed abnormalities of the testis such as severe spermatogenic hypoplasia with Leydig cell hyperplasia (Fig. 1b (ii)) or a focal hypoplastic testis with vacuolar degeneration (Fig. 1b (iii, iv)) in 2/3 male heterozygous (null) KO mice (Cre+), resulting in infertility due to testicular insufficiency. On the other hand, we did not observed abnormalities in female heterozygous (null) KO mice (Cre+). After excision of the Cre cassette, the resultant heterozygous (null) KO mice (Cre-) were very low infertility of male homozygous (null) KO and wild-type mice (Table 1) (polymerase chain reaction [PCR] genotyping of the offspring is shown in Fig. 1c).

Table 1 | Very low fertility of male homozygous (null) KO and wild-type mice from heterozygous (null) KO parents

		Offspring number/parent	
Mouse	Sex	Hetero[a]	Homo[b]
Homozygous KO	Male	0.25	3.10
	Female	0.75	1.80
Heterozygous KO	Male	1.25	-
	Female	2.25	-
Wild-type	Male	0.25	-
	Female	0.25	-

[a]Mating between heterozygous (null) KO mice (Cre−).
[b]mating between homozygous (null) KO mice (Cre−). We obtained offspring from 4 heterozygous (null) KO parents in comparison with those from 10 homozygous (null) KO parents during a 5-month breeding trial.

Homozygous null KO mice. The number of wild-type and MST-KO mice obtained was not sufficient for the planned experiments. Homozygous (null) KO mice used for the present experiment were obtained by mating homozygous (null) KO with homozygous (null) KO. Successful generation was confirmed by the presence of double KO alleles in PCR genotyping (Fig. 2a), no enzyme expression in western blot analyses (Fig. 2b), and no enzymatic activities (data not shown). MST-KO mice showed apparently normal development without male infertility. Macroscopic anomalies were not observed. Furthermore, histological examination with hematoxylin-eosin (HE) staining did not show apparent abnormalities (Fig. 2c). In particular, the layered structure of the cortex in the cerebrum was maintained. In the cerebellum, the cortical structure, including molecular, Purkinje, and granule cell layers of the folia, was maintained. In the liver, hepatic cells around the central vein and the Glisson's sheath of each lobule were normally arranged; and in kidney, the cortical structure, including glomerulus and renal tubules, was normal. Further there is no significant morphological or histological abnormalities in the hippocampus area of the mutants (Fig. 2d).

Behavioral tests. Behavioral tests for MST-KO mice were performed using nonlittermate wild-type mice from 3 different parents as controls. In the open field test, although the total distance and the time spent in the center field tended to be lesser for MST-KO mice than for control mice, significant differences were not observed (Fig. 3a, b). The number of rears did not also differ between the MST-KO and control mice (Fig. 3c). During the test, no functional motor impairment was observed in MST-KO mice. However, as shown in Fig. 3d, during the first 9 min, the distances travelled per minute were lesser for MST-KO mice than for control mice.

The total distance during the first 9 min was 43.3 ± 2.5 m for control mice and 34.2 ± 1.8 m for MST-KO mice ($p = 0.0054$). In particular, during the first 1 minute, the difference between the groups of mice was the largest. MST-KO mice seemed to be strongly hesitating to move when they were put in the novel environment. In the light/dark transition test, the time spent in the light chamber tended to be shorter and the latency of first transition from the dark chamber to the light one tended to be longer for MST-KO mice than for the control mice (Fig. 3e, f). In the elevated plus-maze test, the time spent on the open arms of MST-KO mice was markedly suppressed (Fig. 3g). Therefore, the total distance travelled was also decreased (Fig. 3h). Collectively, the results of these 3 behavioral tests indicate that MST-KO mice show anxiety-like traits[22]. Since the MST-KO mice showed anxiety-like traits, we examined social behavior in the 3-chamber social interaction test to know whether the mice were anxious to contact stranger mice (Fig. 3i). Depressiveness of the MST-KO mice was also examined in the forced swim test, because

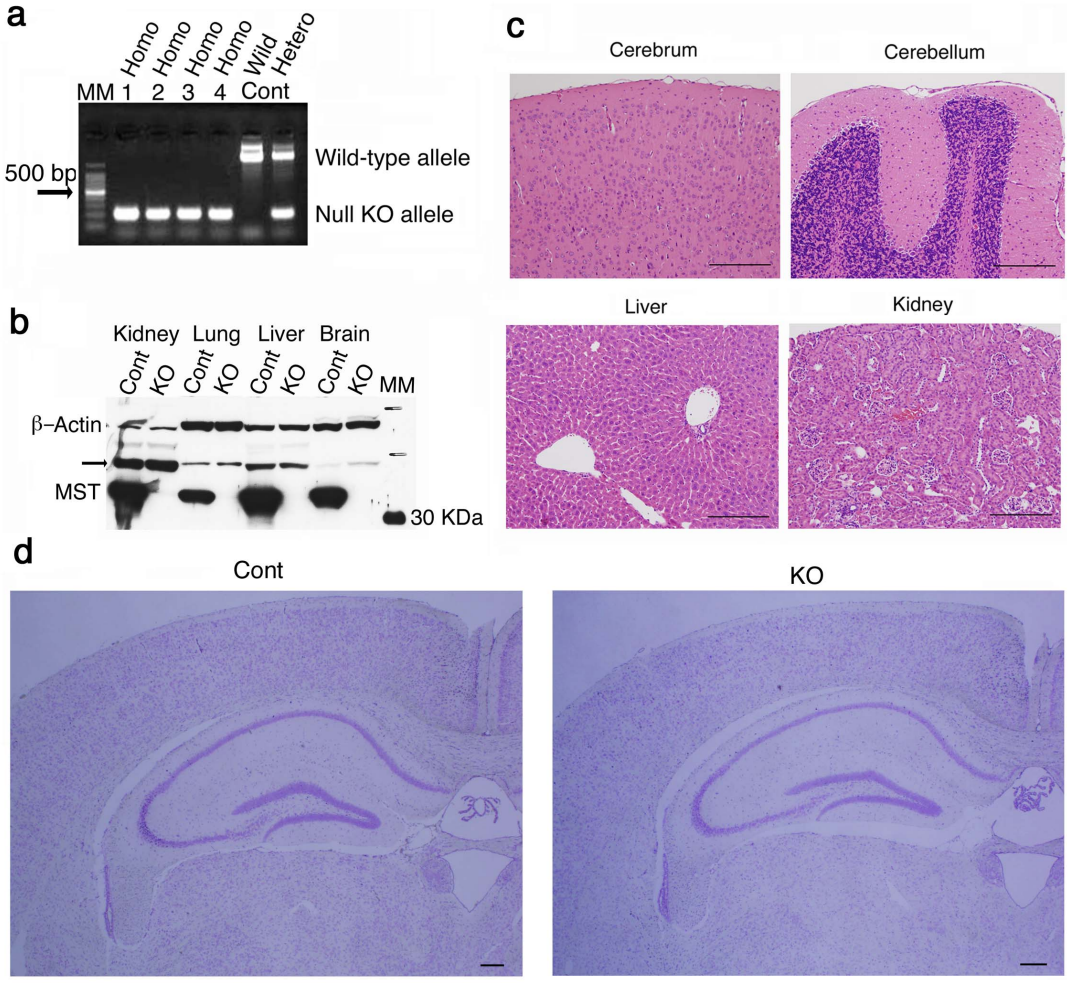

Figure 2 | Homozygous (null) MST-knockout mice. (a) PCR genotyping of offspring produced from mating between MST-KO mice. Genomic DNA was obtained from #44-T-7-3-4-2-8 to 11 (male homozygous) (lanes 1 to 4 in the above order). (b) Western blot analysis for a MST-KO mouse (#44-T-3-2) with overreaction. MM, molecular marker; arrow, rhodanese (the MST antibody slightly cross-reacted with rhodanese); Cont, control mice; KO, MST-KO mice. (c) Microscopic examination (HE staining) of a MST-KO (#44-T-3-2). Bars, 200 μm. (d) Nissl staining for coronal sections of the hippocampal areas of wild-type and the mutant adult brains (#44-H-3-2-1 to 3 and #44-H-3-3-9 to 12). Cont, control mice; KO, MST-KO mice. Bars, 200 μm.

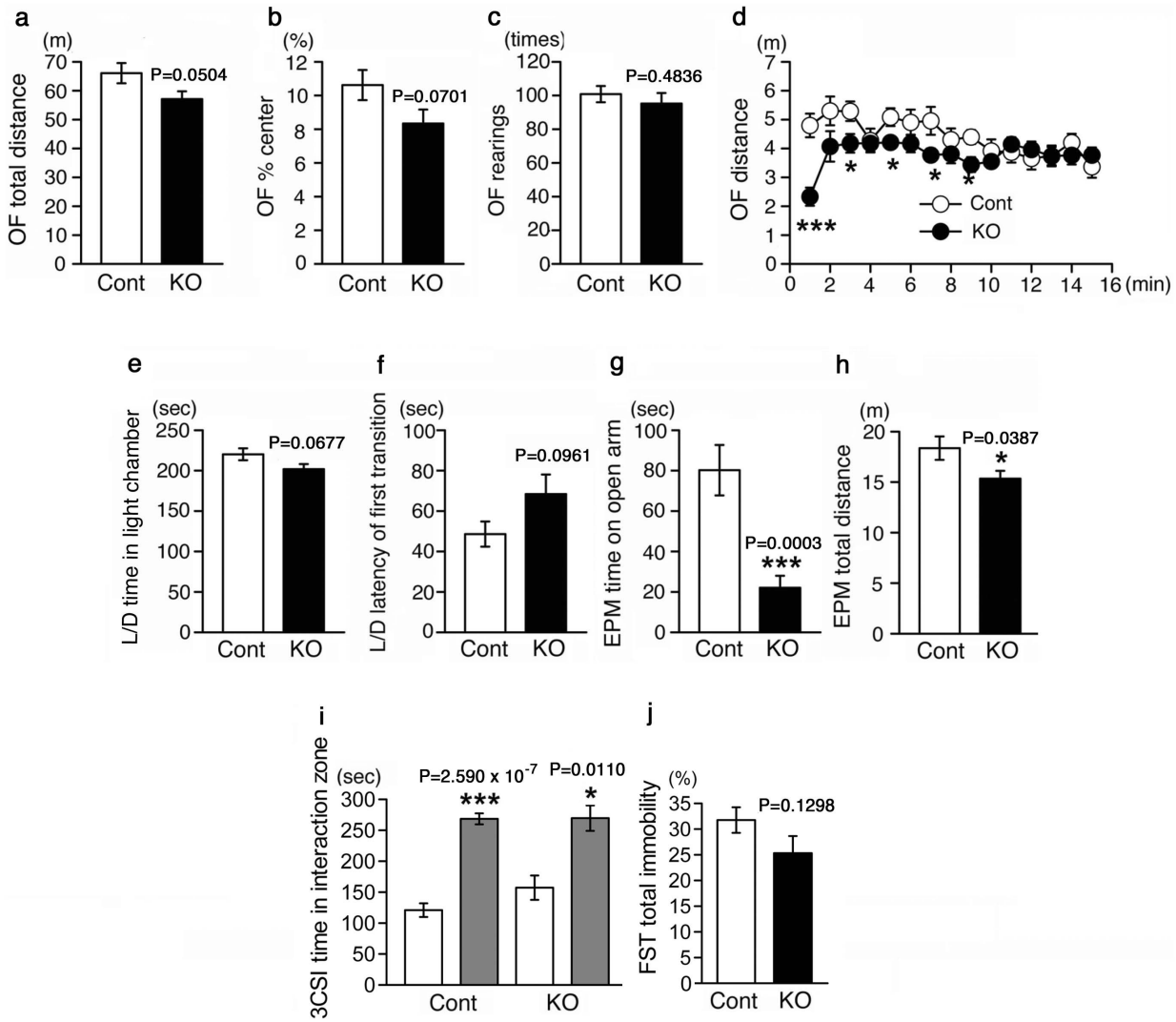

Figure 3 | Behavioral tests. MST-KO mice (#44-H-1-6, 44-H-1-7, 44-H-1-8, 44-H-2-3, 44-H-2-4, 44-H-2-5, 44-H-2-11, 44-H-2-12, 44-H-2-13, 44-H-3-3-1, 44-H-3-3-2, 44-H-3-3-3, 44-H-3-7, 44-H-3-8, 44-H-3-9, 44-H-3-13, and 44-H-3-14 obtained from 6 different parents) showed anxiety-like behaviors (a–h). (a–d) Open field test (OF) (in Fig. 3d, p values of data from 1 to 15 min between MST-KO and control groups are 3.851×10^{-5}, 0.1001, 0.0240, 0.8534, 0.0290, 0.1822, 0.0373, 0.3342, 0.0113, 0.4355, 0.500, 0.5284, 0.9876, 0.3265, and 0.3905, respectively). (e, f) Light/Dark transition test (L/D). (g, h) Elevated plus-maze test (EPM). (i) 3-chambered social interaction tests (3CSI) to examine social behavior. The values of white bars represent the interaction time with empty cage. The values of gray bars represent the interaction time with the cage in which a stranger mouse resides. (j) Forced swim tests (FST) for depressiveness. All data represent the mean ± S.E.M (bar). *, $p < 0.05$; ***, $p < 0.001$; Cont, control mice; KO, homozygous (null) KO mice.

both anxiety and depression can be induced by same pathological background (i.e. impairment of the central serotonergic system) (Fig. 3j). However, no significant differences were observed between MST-KO and control mice in these behavioral tests (Fig. 3i, j).

Quantitative analyses of monoamine and 5-HT_{1A} receptor mRNA. Since increased anxiety-related behaviors in 10 – 12 weeks old MST-KO mice were observed, it is possible that some changes which induce the behavioral abnormalities happens in earlier age. Then, we examined monoamine contests in the PFC (Fig. 4a–d) and hippocampus (Fig. 4e–h) which play important roles in expressing emotion and behaviors. In the PFC, contents of 5-HT and 5-hydroxyindoleacetic acid (5-HIAA), a major metabolite of 5-HT, were increased in null KO mice (Fig. 4b, c). But the 5-HT turnover (5-HIAA/5-HT) was not affected (Fig. 4d). On the other hand, DA content was not different between control and MST-KO mice (Fig. 4a). In the hippocampus, only 5-HIAA content was increased in the MST-KO mice (Fig. 4g). Contents of DA and 5-HT and 5-HT turnover were not different (Fig. 4e, f, h).

On the other hand, quantitative PCR analyses revealed that there were no significant differences in the serotonin $(5\text{-HT})_{1A}$ receptor mRNA levels between control and MST-KO mice in the PCF, hippocampus, and dorsal raphe nucleus (DRN) at the same age (Fig. 5).

Discussion

Human MCDU was reported to be associated with behavioral abnormalities (mental retardation[8-13,15], hypokinetic behavior[8], and grand mal seizures[8]) and anomalies (flattened nasal bridge[8] and excessively arched palate[8]); however, the pathogenesis has not been clarified since MCDU was recognized more than 40 years ago. Macroscopic anomalies were associated in 1 case[8]; however, this could be an accidental combination. We demonstrated that MST deficiency also induced higher brain dysfunction in mice without macroscopic

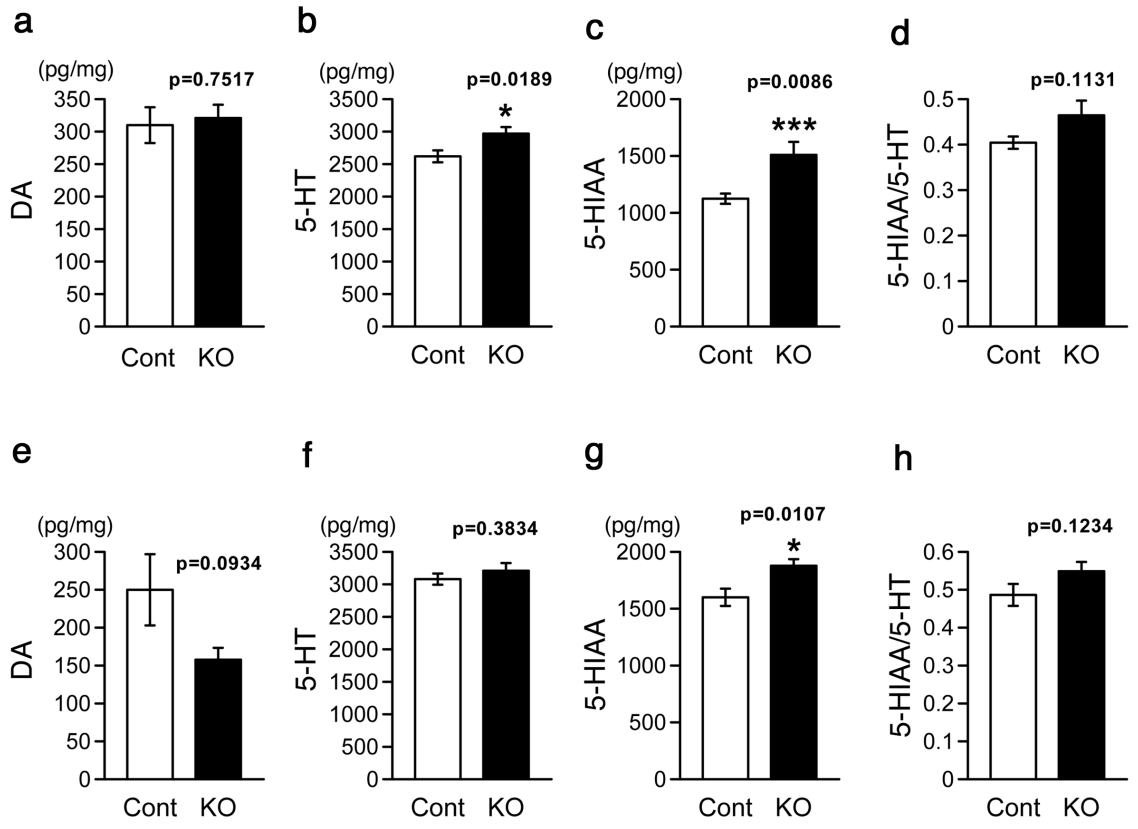

Figure 4 | **Monoamines analyses.** Regional brain monoamines in MST-KO mice (#44-H-2-6-1, 44-H-2-17-1 to 2, 44-H-3-10-1 to 2, and 44-H-3-11-1 to 5 obtained from 4 different parents) were assayed. (a–d) Prefrontal cortex. (e–g) Hippocampus. Monoamine contents were expressed in pg monoamine per mg tissue protein. All data represent the mean ± S.E.M (bar). *, $p < 0.05$; ***, $p < 0.001$; Cont, control mice; KO, homozygous (null) KO mice.

and microscopic abnormalities in the brain. From the results of the behavioral tests, MST seems to play a critical role in the central nervous system, i.e., to establish normal anxiety.

The expression levels of MST in the brain during the fetal and postnatal periods are higher than those in the adult brain (unpublished data) although the promoter region shows characteristics of a typical housekeeping gene[23]. This observation is supported by the finding that MST expression in the cerebellum is decreased during the adult period[24]. On the other hand, the MST expression level in the lung decreases from the perinatal period (unpublished data). These facts suggest that MST could function in the fetal and postnatal brain.

It was reported that serotonin signaling via the 5-HT_{1A} receptor in the brain during the early developmental stage plays a critical role in the establishment of innate anxiety during the early developmental stage[25,26]. Indeed, changes in contents of 5-HT and 5-HIAA were observed in the PFC and hippocampus of the MST-KO mice at the age before the behavioral abnormalities observed, while there was no, differences in 5-HT_{1A} mRNA expression in the PFC, hippocampus, and dorsal raphe nucleus at the same age. It remains unclear whether the apparent increase in serotonin signaling are causally related to anxiety-related behaviors[26]. The increase in serotonin may interfere with normal brain development or may reflect compensation of

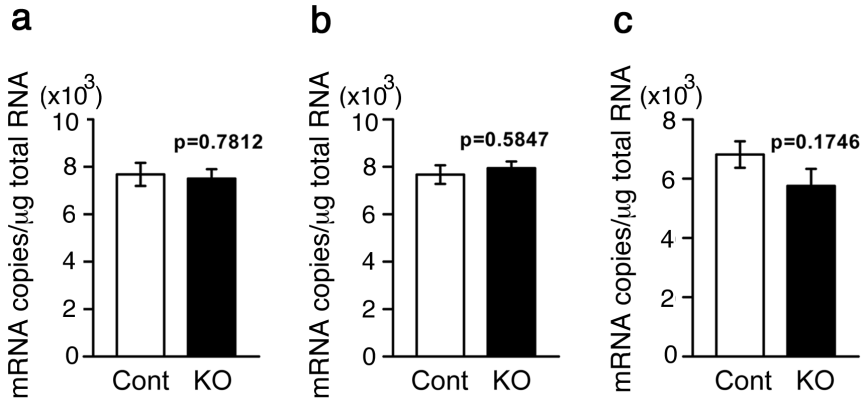

Figure 5 | **Quantitative analyses of $5HT_{1A}$ receptor mRNA.** Regional brain $5HT_{1A}$ receptor mRNA in MST-KO mice (for the PFC and hippocampus were from #44-H-2-6-1, 44-H-2-17-1 to 2, 44-H-3-10-1 to 2, and 44-H-3-11-1 to 5 obtained from 4 different parents; for DRN were from #44-H-3-10-4-1 to 3, and 44-H-2-17-3-1 to 7 obtained from 2 different parents) were assayed. (a) PFC. (b) Hippocampus. (c) DRN. Amount of $5HT_{1A}$ receptor mRNA were expressed in copies per μg tissue total RNA. All data represent the mean ± S.E.M (bar). Cont, control mice; KO, homozygous (null) KO mice.

reduced signaling pathway downstream of serotonin receptors. Alternatively, 5-HT receptors other than 5-HT_{1A} may be involved in the behavioral abnormalities in MST-KO mice.

Here, we propose 2 hypotheses on the pathogenesis of anxiety in MST-KO mice. First, the symptoms would be caused by failure of recapitulation of phylogenesis of central nervous system in ontogenesis due to lack of MST, which serves as an antioxidant. Immunohistochemical study using anti-MST antibody in adult rat cerebrum revealed that glial cells were positively staining, but the neural cells were not remarkably stained[2].

In rat MST, MST possesses 2 redox-sensing molecular switches[3,5]. A catalytic-site cysteine and an intersubunit disulfide bond serve as a thioredoxin-specific molecular switch[3,5]. The intermolecular switch is not observed in prokaryotes and plants, which emerged into the atmosphere under reducing conditions[4]. As a result, MST acquired different functions such as a redox regulation (maintenance of cellular redox homeostasis) and defense against oxidative stress, in the atmosphere under oxidizing conditions.

On the other hand, MST can produce H_2S (or HS^-) as a biofactor[6], which cystathionine β-synthase[27] and cystathionine γ-lyase[28] also can generate. Interestingly MST can uniquely produce SO_x in the redox cycle of persulfide formed at the low-redox catalytic-site cysteine[7]. As an alternate hypothesis on the pathogenesis of the symptoms, H_2S (or HS^-) and/or SO_x could suppress anxiety-like behavior, and therefore, defects in these molecules could increase anxiety-like behavior. However, no microanalysis method has been established to quantify H_2S (or HS^-) and SO_x at the physiological level. We are currently developing the required in vivo technique.

Methods

Knockout mice production. The MST targeting vector covered a region from the initiation codon ATG (A was referred to as 1 bp) in exon 1 to 3608 bp in exon 2, including the introns, on mouse chromosome 15 (NC_000081) (Fig. 1a). The long arm included the promoter region (from -5977 bp to the initiation codon, ATG), and the short arm included a region from 3608 to 6533 bp. A *loxP* site was inserted prior to the initiation codon, ATG, and the FRT-neo-FRT-*loxP* sequence was inserted prior to position 3608 bp of exon 2. Functional expression of a Cre/*loxP* site-specific recombination system to generate tissue-specific (conditional) and null KO mice[17,20,21] was applied for gene targeting. These vectors were transfected into ES cells derived from C57BL/6 mice (Bruce-4 ES cells, UNITECH Co., Ltd., Chiba, Japan) via electroporation.

After neomycin-treated culture, colonies obtained by gene disruption through homologous recombination were selected by PCR genotyping and Southern blot analysis. To confirm the presence of the *loxP* sequence between exon 1 and the long arm, PCR genotyping was performed using a forward primer (long-F probe: GCTTGTCTCTCCATTCTGGTATCTT) on the long arm and a reverse primer (exon-R probe: AGACACCAGAGCTCGGAAAAGTT) on exon 1 (Fig. 1a). Further, to confirm homologous recombination, Southern blot analysis was performed using a 3′-probe (289 bps) binding on the long arm, a 5′-probe (265 bps) binding upstream on the short arm, and a neomycin probe (694 bps) binding in the neo sequence (Fig. 1a). The chimeric ES cells were injected into blastocysts derived from wild-type Balb/c mice (UNITECH Co., Ltd., Chiba, Japan), which were transplanted into host ICR mice (UNITECH Co., Ltd., Chiba, Japan) to generate chimeric mice.

Male chimeric mice were mated with wild-type female C57BL/6J mice (CLEA Japan, Inc., Tokyo, Japan) to obtain F1 male mice, which were mated with wild-type female C57BL/6J mice again to obtain F2 mice (flox mice; heterozygous targeting sequence knock-in mice). To confirm homologous recombination, PCR genotyping was performed using a forward primer (neo-F probe: CGTGCAATCCATCTTGT TCAAT) binding on the neo sequence and a reverse primer (up-R probe: TCCAGT AGACAAAAACTCTGCTCAC) binding upstream of the short arm (Fig. 1a).

To confirm the presence of the *loxP* sequence between exon 1 and the long arm, PCR genotyping was performed using a long-F probe and an exon-R probe as described above.

Then, to generate heterozygous (null) KO mice containing the Cre cassette, heterozygous knock-in mice were mated with transgenic mice (Cre expression in the whole tissues). To confirm the knockout allele, PCR genotyping was performed using a forward primer (long-F probe) and a reverse primer (short-R probe: CTGGTACTGTGATGGTCAGATGTC), binding on the short arm (Fig. 1a). The exon-R probe was used to confirm deletion of the exon sequence. Because the male heterozygous KO mice with the Cre cassette were frequently infertile, the Cre cassette was excised by mating those mice with wild-type mice (C57BL/6J). The excision was confirmed by PCR genotyping using a forward primer (Cre-F probe: CGCGATTATCTTCTATATCTTCAGG) and a reverse primer (Cre-R probe: AGGTAGTTATTCGGATCATCAGCTA), binding on the Cre cassette. However, male heterozygous KO mice without the Cre cassette were also frequently infertile. Thus, homozygous KO mice used for the present experiment were obtained from mating homozygous KO mice with homozygous KO mice.

PCR for genotyping. PCR was performed using LA Taq with GC buffer (Takara Bio Inc., Shiga, Japan). Genomic DNA was extracted from each mouse-tail. The cycling parameters for PCR were as follows: for the first segment, 1 cycle of denaturation at 94°C for 2 min and for the second segment, 35 cycles of denaturation at 94°C for 20 s, annealing at 62°C for 6.5 min, and extension at 72°C for 10 min.

Western blot analysis. Experimental and wild-type mice were deeply anesthetized by intra-abdominal pentobarbital injection (100 mg/100 g body weight), and killed by exsanguination. The organs, including the brain, lung, liver, kidney, and testis or ovary were excised. All methods, including preparation of the used anti-rat MST polyclonal antibody and tissue homogenate for western blotting, were as described previously[2,18], except for the use of an sodium dodecyl sulfate-polyacrylamide gel (12.5%) and the amount of loaded protein from each homogenate per lane (10 μg).

Microscopic examination. After excision of organs as described above, the organs were fixed by perfusion of phosphate-buffered 10% formaldehyde (pH 7.3). The tissues were embedded in paraffin and hematoxylin-eosin staining was performed. For precise examination for mouse brains, they were fixed with 4% paraformaldehyde by perfusion, processed as paraffin-embedded samples and sectioned at 6 μm. Serial sections on slide glasses were stained with 1% cresyl violet and analyzed using an Olympus BX52 microscope equipped with DP70 digital photomicrograph system.

Behavioral tests. All behavioral tests were performed between 0830 hours and 1400 hours using male MST-KO mice (between 10 and 12 weeks old; n = 17 per group). The MST-KO mice were obtained from 6 different parents. The control wild-type mice (C57BL/6J) were purchased from Japan SLC, Inc. (Shizuoka, Japan), not from littermates (from 3 different parents), because we hardly obtained offspring owing to frequent male infertility of heterogynous KO mice as described above. The apparatuses and software for imaging and analyzing used in the present study were products of O'Hara & Co. Ltd. (Tokyo, Japan). Open field tests were performed prior to other behavioral tests. The plastic open-field chamber was 50 (length) × 50 (width) × 50 cm (height). The field was illuminated at 40 lux. Behavior was monitored for 15 min and recorded by a CCD camera connected to a personal computer. The ambulation distance, number of rears, and percentage of time spent in the center of the field were recorded automatically using Image OF software. The center of the field was defined as a central square of 30 cm × 30 cm. Light/dark transition test was performed after the open-field test.

The apparatus used for the light/dark transition test consisted of a cage (21 × 42 × 25 cm) divided into 2 sections of equal size by a partition with a door. One chamber was brightly illuminated (600 lux), whereas the other chamber was dark (8 lux). Mice were placed on the dark side, and allowed to move freely between the 2 chambers with the door being open for 10 min. Time spent on each side and first latency to the light side were recorded automatically using Image LD software. The elevated plus-maze test was then performed and it consisted of 2 open arms (25 × 5 cm) and 2 closed arms of the same size, with 15-cm-high transparent walls. The arms and central square were made of white plastic plates and were elevated to a height of 55 cm above the floor. Arms of the same type were arranged at opposite sides to each other. Each mouse was placed in the central square of the maze (5 × 5 cm), facing 1 of the closed arms. Mouse behavior was recorded during a 10-min test period. Time spent on open arms was recorded. Data acquisition and analysis were performed automatically, using Image EP software.

For 3-chambered social interaction test, the apparatus used for the test was plastic box (40 × 60 × 20 cm) with two partitions separating the box into 3 same size chambers. The box was illuminated at100 lux and the partitions have openings that allow the mouse freely from one chamber to another. At the left corner of the left chamber, an empty wire cage (11 cm height × 9 cm diameter) was placed. At the right corner of the right chamber, the same wire cage in which an unfamiliar younger wild-type male mouse was placed. At the beginning of the test, the test mouse was placed in the middle chamber and then the mouse can move freely throughout all 3 chambers. During 10 min session the behavior was recorded and the time spent in the interaction zone, within 9 cm from the edge of the wire cage, was measured automatically using Image CSI software.

In Forced swim test, on the first day (training day), mice were placed into the plexiglas cylinders (20 cm height × 10 cm diameter) filled with water (25°C), up to a height of 7.5 cm for 15 min. On the second day (testing day), 24 hours after the training, mice were placed into the plexiglas cylinders filled with water (25°C) again, their behavior was recorded over a 6-min test period. Data acquisition and analysis were performed automatically, using Image PS software. Immobility was measured by Image PS software using stored image files.

Monoamine analyses. Brain tissue concentrations of dopamine (DA), serotonine (5-HT) and 5-Hydroxyindoleacetic acid (5-HIAA) were measured by a high performance liquid chromatography (HPLC) system (Eicom, Japan) (n = 9–10 per group). The brain tissues of 5 weeks old mice were used. Details of the procedure used here is previously descrived[26].

Quantitaive analyses of 5-HT_{1A} receptor mRNA. Brain tissues of 5 weeks old mice were used and TaqMan (Life technologies, USA) assay was employed (n = 8–10 per group). Details of the procedure used here is previously descrived[26]. The sequences of

the forward primer, reverse primer, and TaqMan probe for mouse 5-HT_{1A} receptor were 5′-AATTATTGGCTCGGTCTTTGG-3′, 5′- CGTGAAGAATTGGGATT TCG-3′, and 5′- TCAGTTTTGATAGTTGCAATAACCTCC -3′, respectively.

Statistical analysis. In Fig. 3, 4, 5, except the data of Fig. 3i, differences between the control and MST-KO mice were analyzed by unpaired Student's *t* test using SPSS Statistics (IBM Co., New York, USA). In Fig. 3i, differences in the time between the empty cage and the stranger mouse were analyzed by paired Student's *t* test using SPSS Statistics. All values are presented as mean ± standard error. A p value of less than 0.05 was considered to indicate statistical significance.

Animal experiments. All experiments were performed in accordance with guidelines and regulations for the Care and Use of Laboratory Animals, Nippon Medical School.

1. Jarabak, R. 3-Mercaptopyruvate sulfurtransferase. *Methods Enzymol.* **77**, 291–297 (1981).
2. Nagahara, N., Ito, T., Kitamura, H. & Nishino, T. Tissue and subcellular distribution of mercaptopyruvate sulfurtransferase in the rat: confocal laser fluorescence and immunoelectron microscopic studies combined with biochemical analysis. *Histochem. Cell Biol.* **110**, 243–250 (1998).
3. Nagahara, N. & Katayama, A. Post-translational regulation of mercaptopyruvate sulfurtransferase via a low redox potential cysteine-sulfenate in the maintenance of redox homeostasis. *J. Biol. Chem.* **280**, 34569–34576 (2005).
4. Nagahara, N. Regulation of Mercaptopyruvate sulfurtransferase activity via intrasubunit and intersubunit redox-sensing switches. *Antioxid. Redox Signal.* (2013) in press (2012 Dec 19. [Epub ahead of print]).
5. Nagahara, N., Yoshii, T., Abe, Y. & Matsumura, T. Thioredoxin-dependent enzymatic activation of mercaptopyruvate sulfurtransferase. An intersubunit disulfide bond serves as a redox switch for activation. *J. Biol. Chem.* **282**, 1561–1569 (2007).
6. Shibuya, N. *et al.* 3-Mercaptopyruvate sulfurtransferase produces hydrogen sulfide and bound sulfane sulfur in the brain. *Antioxid. Redox Signal.* **11**, 703–714 (2009).
7. Nagahara, N., Nirasawa, T., Yoshii, T. & Niimura, Y. Is novel signal transducer sulfur oxide involved in the redox cycle of persulfide at the catalytic site cysteine in a stable reaction intermediate of mercaptopyruvate sulfurtransferase? *Antioxid. Redox Signal.* **16**, 747–753 (2012).
8. Ampola, M. G., Efron, M. L., Bixby, E. M. & Meshorer, E. Mental deficiency and a new aminoaciduria. *Am. J. Dis. Child.* **117**, 66–70 (1969).
9. Crawhall, J. C. *et al.* Beta mercaptolactate-cysteine disulfide: analog of cystine in the urine of a mentally retarded patient. *Science* **160**, 419–420 (1968).
10. Crawhall, J. C., Parker, R., Sneddon, W. & Young, E. P. Beta-mercaptolactate-cysteine disulfide in the urine of a mentally retarded patient. *Am. J. Dis. Child.* **117**, 71–82 (1969).
11. Crawhall, J. C., Bir, K., Purkiss, P. & Stanbury, J. B. Sulfur amino acids as precursors of beta-mercaptolactate-cysteine disulfide in human subjects. *Biochem. Med.* **5**, 109–115 (1971).
12. Crawhall, J. C., Purkiss, P. & Stanbury, J. B. Metabolism of sulfur-containing amino acids in a patient excreting -mercaptolactate-cysteine disulfide. *Biochem. Med.* **7**, 103–111 (1973).
13. Crawhall, J. C. A review of the clinical presentation and laboratory findings in two uncommon hereditary disorders of sulfur amino acid metabolism, beta-mercaptolactate cysteine disulfiduria and sulfite oxidase deficiency. *Clin. Biochem.* **18**, 139–142 (1985).
14. Niederwiesler, A., Giliberti, P. & Baerlocher, K. Beta-mercaptolactate cysteine disulfiduria in two normal sisters. Isolation and characterization of beta-mercaptolactate cysteine disulfide. *Clin. Chem. Acta* **43**, 405–416 (1973).
15. Law, E. A. & Fowler, B. Beta-mercaptolactate cysteine disulphiduria in a mentally retarded Scottish male. *J. Ment. Defic. Res.* **20**, 99–104 (1976).
16. Hannestad, U., Mårtensson, J., Sjödahl, R. & Sörbo, B. 3-mercaptolactate cysteine disulfiduria: biochemical studies on affected and unaffected members of a family. *Biochem. Med.* **26**, 106–114 (1981).
17. Nagahara, N. & Ito, T. MST knockout mouse production and comprehensive analyses. In abstract of the 83rd Annual meeting of Japanese Biochemistry Society. 183 (2010).
18. Nagahara, N., Okazaki, T. & Nishino, T. Cytosolic mercaptopyruvate sulfurtransferase is evolutionarily related to mitochondrial rhodanese: striking similarity in active site amino acid sequence and the increase in the mercaptopyruvate sulfurtransferase activity of rhodanese by site-directed mutagenesis. *J. Biol. Chem.* **270**, 16230–16235 (1995).
19. Nagahara, N. & Nishino, T. Role of amino acid residues in the active site of rat liver mercaptopyruvate sulfurtransferase. cDNA cloning, overexpression, and site-directed mutagenesis. *J. Biol. Chem.* **271**, 27395–27401 (1996).
20. Le, Y. & Sauer, B. Conditional gene knockout using cre recombinase. *Methods Mol. Biol.* **136**, 477–485 (2000).
21. Chiang, P. M. *et al.* Deletion of TDP-43 down-regulates Tbc1d1, a gene linked to obesity, and alters body fat metabolism. *Proc. Natl. Acad. Sci. USA* **107**, 16320–16324 (2010).
22. Crawley, J. N. Emotional behaviors: animal models of psychiatric diseases. in *What's wrong with my mouse? Behavioral phenotyping of transgenic and knockout mice.* 226–265, 2nd edn., (John Wiley & Sons, New Jersey, 2007).
23. Nagahara, N. *et al.* A point mutation in a silencer module reduces the promoter activity for the human mercaptopyruvate sulfurtransferase. *Biochim. Biophys. Acta* **1680**, 176–184 (2004).
24. Shibuya, N. *et al.* A novel pathway for producing hydrogen sulfide from D-cysteine. *Nat. Commun.* **4**: 1366 doi: 10.1038/ncomms2371 (2013).
25. Richardson-Jones, J. W. *et al.* Serotonin-1A autoreceptors are necessary and sufficient for the normal formation of circuits underlying innate anxiety. *J. Neurosci.* **31**, 6008–6018 (2011).
26. Nagano, M. *et al.* Early intervention with fluoxetine reverses abnormalities in the serotonergic system and behavior of rats exposed prenatally to dexamethasone. *Neuropharmacol.* **63**, 292–300 (2012).
27. Abe, K. & Kimura, H. The possible role of hydrogen sulfide as an endogenous neuromodulator. *J. Neurosci.* **16**, 1066–1071 (1996).
28. Hosoki, R., Matsuki, N. & Kimura, H. The possible role of hydrogen sulfide as an endogenous smooth muscle relaxant in synergy with nitric oxide. *Biochem. Biophys. Res. Commun.* **237**, 527–531 (1997).

Acknowledgements

We thank Y. Mikahara (Department of Pharmacology, Nippon Medical School) for technical assistance in the behavioral tests and also T. Maeda (Department of Pathology and Experimental Medicine, Kumamoto University) for technical assistance in the morphological studies. This study was supported by a Grant-in-Aid for Scientific Research from the Ministry of Education, Science and Culture of Japan (24580392).

Author contributions

N.N. managed the project, designed experiments, and produced KO mice. M.N. and H. S. designed and performed behavioral tests. They also performed monoamine and 5-HT_{1A} receptor analyses. T. I. performed examinations in developmental biology and pathology. K. S. performed macroscopic and microscopic examinations of the brain. T. A. cared and bred the KO mice. All authors reviewed the final manuscript.

Additional information

Competing financial interests: The authors declare no competing financial interests.

How to cite this article: Nagahara, N. *et al.* Antioxidant enzyme, 3-mercaptopyruvate sulfurtransferase-knockout mice exhibit increased anxiety-like behaviors: a model for human mercaptolactate-cysteine disulfiduria. *Sci. Rep.* **3**, 1986; DOI:10.1038/srep01986 (2013).